Transactions of the 15th International Conference on
Structural Mechanics in Reactor Technology (SMiRT-15)
Seoul, Korea, August 15-20, 1999

CFD Analysis of Turbulent Flows in Rod Bundles for Nuclear Fuel Spacer Design

Wang Kee In, Tae Hyun Chun, Dong Seok Oh and Yeon Ho Jung

Korea Atomic Energy Research Institute, Korea

ABSTRACT : A CFD analysis was performed to confirm the applicability of the CFD method and to examine the 3-D turbulent flow characteristics in rod bundles with a typical flow mixing promoter on a grid spacer. Two experiments with "split vane" and "ripped-open" blades were simulated in this CFD study. Both the split vane and ripped-open type mixing promoters have two mixing blades on top of the spacer and bent in opposite directions that produce a swirling flow in the subchannel as well as a crossflow between the adjacent subchannels. The CFD predictions were compared with the measurements to evaluate the applicability of the CFD analysis to the nuclear fuel-spacer design. The CFD results presented the detailed characteristics of turbulent flow in rod bundles well and showed good agreement with the measurements. The CFD method was confirmed to be quite useful for the optimal design of grid spacers.

INTRODUCTION

The fuel element geometry typically used in nuclear reactors is the rod bundle whose rod-to-rod clearance is maintained by the grid spacer. The heat generated in the rods by the nuclear reaction is removed by the coolant, usually in turbulent flow. The coolant moves axially through the subchannels formed between neighboring fuel rods and between the peripheral fuel rods and the flow tube. One component of a fuel rod bundle is the grid spacer that maintains an appropriate rod-to-rod clearance. The fuel spacer affects the coolant flow distribution in a fuel rod bundle, and so spacer geometry has a strong influence on a bundle's thermal-hydraulic characteristics, such as critical heat flux and pressure drop. The flow mixing devices on the grid spacer would enhance the mixing rate between subchannels and promote turbulence in the subchannel. The forced mixing effects appeared to be strong near the spacer but were shown to suddenly decay downstream of the spacer. The fuel-grid spacer with flow mixing devices should therefore be designed to maintain a high mixing rate and turbulence further downstream to improve the DNB performance of fuel-rod bundles without resulting in an excessive pressure drop. It is therefore essential to evaluate the turbulent flow characteristics in detail for the optimal design of the grid spacer with flow mixing devices. Since the optimal spacer design should consider tremendous shapes and sizes of mixing blades on the grid spacer, the utilization of the CFD method is inevitable to sift better fuel-spacer designs for the final experimental verification. The previous CFD predictions of turbulent flows in rod bundles with mixing devices on the spacer have reported that the CFD predictions are in good agreement with experimental data and quite effective for designing

fuel grid spacers with mixing devices.

The prediction of the detailed structure of turbulent flow in rod bundles, used especially as nuclear fuel elements, is required to ensure their safe and reliable operation. The experimental data on flow mixing between the subchannels of bare rod bundles (Rowe *et al.*, 1974; Moller, 1991; Rehme, 1992) showed that the almost periodical flow pulsations between subchannels are the main mechanism for the natural mixing between subchannels resulting from radial pressure gradients between adjacent subchannels. The presence of the grid spacer and flow mixing devices causes the forced mixing of coolant that promotes flow mixing either within a subchannel or between subchannels. Shen *et al.* (1991) investigated the crossflow mixing effect caused by the grid spacer with ripped-open blades. They measured the crossflow velocity and the RMS velocity at the rod gap region depending on the angle of the mixing blade on the grid spacer. Yang and Chung (1996) measured turbulent flow characteristics in subchannels of 5x5 rod bundles with mixing vanes and found that the turbulent mixing and forced mixing occurs behind the grid spacer. Imaizumi *et al.* (1995) developed a CFD method to evaluate 3-D flow characteristics for PWR fuel assembly in order to improve the design approach. Karoutas *et al.* (1995) performed a 3-D flow analysis for the design of a nuclear fuel spacer by CFD and experimental methods. A CFD analysis was performed here to confirm the applicability of the CFD method and to investigate the characteristics of turbulent flow in rod bundles with flow mixing devices on the grid spacer. Two experiments with split vane and ripped-open blades were simulated in this CFD study.

CFD MODELING AND ANALYSIS

Two different experiments with flow mixing promoters (split vane and ripped-open blades) are simulated in this study for CFD applications. Karoutas *et al.* (1995) reported the axial and lateral velocity measurements taken at the centerline across adjacent subchannels for the split-vane design. The split-vane design shown in Fig. 1 places two blades on top of the spacer bent in opposite directions to produce a swirling flow pattern in the subchannel. Figure 1 also shows an array of rods with the spacer to demonstrate flow patterns in adjacent subchannels (P/D=1.33, D=9.53 mm). Shen *et al.* (1991) performed the LDV measurements on the distributions of transverse mean velocity and RMS velocity for flow through a sixteen-rod bundle (P/D=1.375, D=6 mm) with ripped-open blades on the grid spacer shown in Fig. 2.

A single subchannel of one grid span is modeled using flow symmetry by a CFD code, CFX(AEA Technology, 1997). The spacer and mixing devices are treated as infinite thin surfaces, and other fuel spacer elements such as spring and arches are typically neglected for simplicity. The dimensions of the split vane and the ripped-open blades are assumed based on an engineering judgement because they are not known. The bent angle of the mixing blades is assumed to be 25° from the axial flow direction. The CFD simulation starts 45-65 mm upstream and 500 mm downstream of the top of the grid spacer. The inlet boundary conditions used in the simulations were taken from a model without a spacer. Velocities, turbulent kinetic energy and turbulent dissipation rate were transferred from the outlet in the no spacer case to the inlet in the simulations with spacers. The working fluid is water at the respective experimental conditions. The average inlet velocities are 6.79 m/sec (Re=65000) for the split-vane design and 2.5 m/sec (Re=14200) for the ripped-open blades.

A pressure boundary condition was applied at the outlet with constant pressure in the cross-section of the subchannel. Special periodic boundary conditions at the rod gap regions were used to model the crossflow between neighboring subchannels and reduce the size of the computational model. What is coming out through one side boundary is going in through another side boundary in the computational model. The computational grid for the one grid

span of a single subchannel is approximately 250000 cells and the fine grid was used near the grid spacer and the rod surfaces. The standard $k-\varepsilon$ turbulence model of Launder and Spalding (1974) was used in this simulation since it is widely used and converges well. A standard under-relaxation method and HYBRID difference scheme were used to obtain a converged solution. The calculation was performed on HP9000 C200 (PA8000 CPU, 512 MB RAM) and terminated when the residuals for all governing equations were reduced by a factor of 10^3 to 10^4. Approximately 4000 to 5000 iterations were needed to obtain a converged solution.

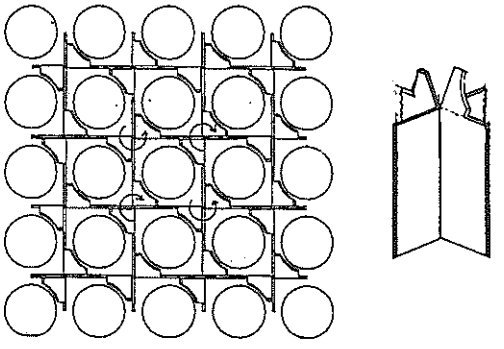

Fig. 1 Schematic of flow pattern and split-vane design (Karoutas *et al.* 1995)

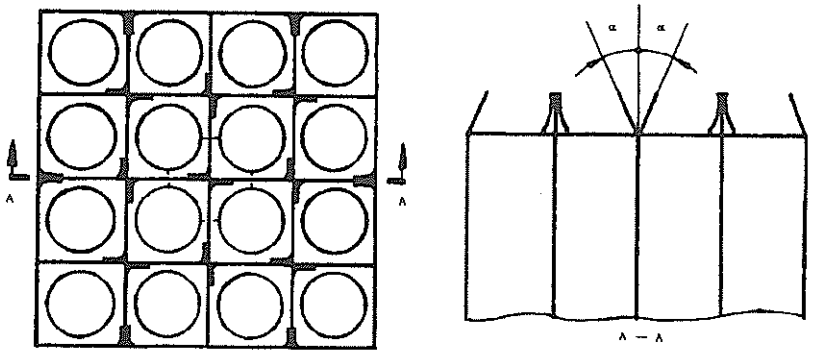

Fig. 2 Arrangement of ripped-open blades (Shen *et al.* 1991)

RESULTS AND DISCUSSIONS

The CFD predictions of the axial and transverse velocities of mean flow and the turbulent kinetic energy were made for 3-D turbulent flows in rod bundles with the split vane and the ripped-open blades on the grid spacer. The CFD predictions show that the split vane generates primarily a swirling flow pattern in the subchannel (Fig. 3a), but the ripped-open blades produce a crossflow between subchannels with a weak swirling flow in the subchannel (Fig. 3b). The swirl and the transverse mean velocity tend to decrease downstream of the grid spacer.

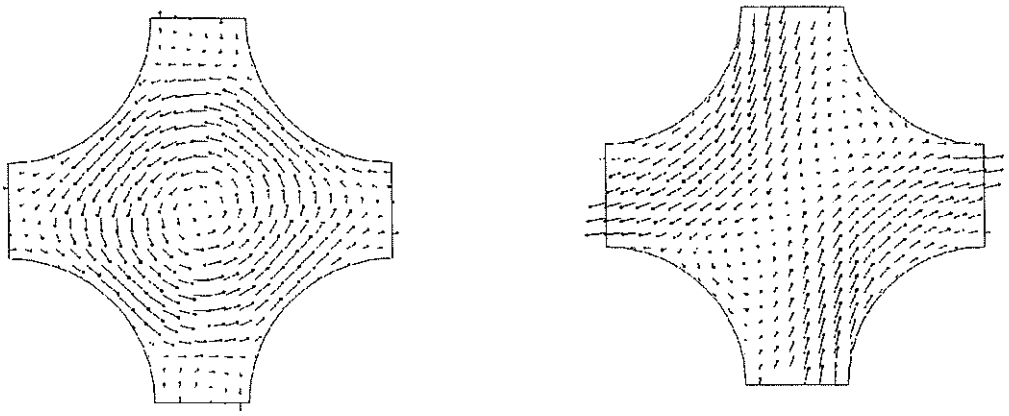

(a) (b)

Fig. 3 Flow pattern in subchannel at z/D_h=7; (a) split vane, (b) ripped-open blades

Axial and Lateral Mean Velocities

The axial and lateral mean velocities were predicted along the centerline of subchannel and compared to the measurements (Karoutas *et al.*, 1995). The velocities are normalized by the bulk velocity in subchannel (V_{avg}=6.79 m/sec). Figure 4 shows the comparison of the axial velocity across the width of two subchannels downstream of the grid spacer with split vane. There are some significant differences between the predictions and the measurements close to the spacer. These larger differences are mainly due to the thickness of the spacer strip and the rod support features of the spacer such as springs and arches which are not modeled in the CFX model. The comparison shows qualitatively good agreement further downstream of the spacer ($z/D_h \geq 8.5$). A large variation in axial velocity across the subchannel is noted near the spacer ($z/D_h \leq 4.2$) and the distribution of axial velocity develops to the parabolic profile in both measurements and predictions. Far downstream ($z/D_h \geq 26.5$) the predicted axial velocities show a more developed (parabolic) shape than the measurements show. This may be due to not modeling the next spacer at the outlet of the CFX model. The next spacer was not modeled to minimize the size and execution of the CFD simulation. The next spacer would have a damping effect on the centerline subchannel velocity. Figure 5 shows the results of comparison of the lateral velocity along the centerline across two subchannels for the split-vane design. It can be seen that the lateral velocity produced by split vane is high close to the spacer but decreases significantly further downstream. The predicted lateral velocities show good agreement with the measurements. The slight under-prediction appears to be caused mainly by inexact dimensions of split vane. Modeling of multi-subchannels would somewhat enhance the accuracy of the predictions.

A swirl ratio was calculated to compare the magnitude of swirl in subchannel. The swirl ratio is defined as

$$F_{CHAN} = \frac{1}{2P} \int \frac{|V|}{V_{avg}} ds \,. \tag{1}$$

Where P is a pitch and V is the lateral velocity perpendicular to the centerline across two subchannels. The swirl ratio was calculated at all measuring heights downstream of the spacer and compared to the measured results (Karoutas *et al.*, 1995) in Fig. 6. The predicted swirl ratios in the axial direction are slightly lower than the measurements but well indicate the characteristics of the swirling flow generated by the split vane. The under prediction is

due to the uncertainty in the dimensions of the split vane and the use of the standard $k-\varepsilon$ turbulence model. The $k-\varepsilon$ model is known to not accurately model high swirling flow. A strong swirling flow appears to occur close to the split vane but rapidly changes to the axially dominant flow further downstream. The predicted swirl ratio decreased to below 5% of the bulk velocity at z/D_h=15.0. Increasing the swirl ratio and its persistence downstream of the spacer is believed to improve DNB performance.

Figure 7 shows the transverse velocity distributions on a rod gap region of central subchannel for the ripped-open blades. The positive velocity means the inflow to subchannel and vice versa. Both the measured and predicted transverse velocities rapidly decrease downstream of the spacer. It can be noted that the velocity inversion (change in the direction of crossflow) appears in the measurements near the spacer ($7< z/D_h <13$) but not in the CFD predictions. The predicted crossflow rate is also slightly smaller than the measured one. These discrepancies are judged to be due to the effects of uncertainty in blade, adjacent subchannels and outer wall boundary in the experiment. The central subchannel only was modeled with an assumed size of the blade in this CFD analysis. However, overall agreement at some distance downstream ($z/D_h>13$) appears to be reasonable.

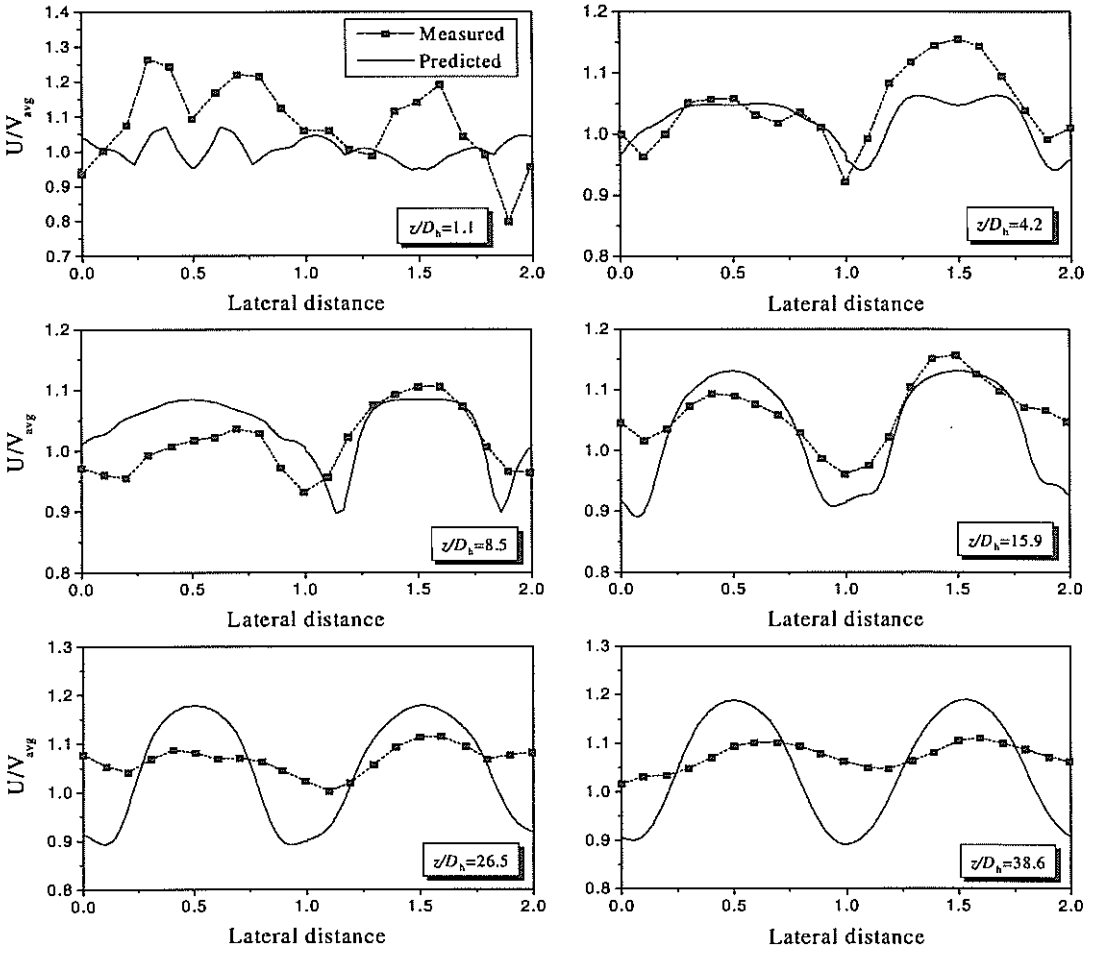

Fig. 4 Axial velocity along the centerline of subchannel for split vane

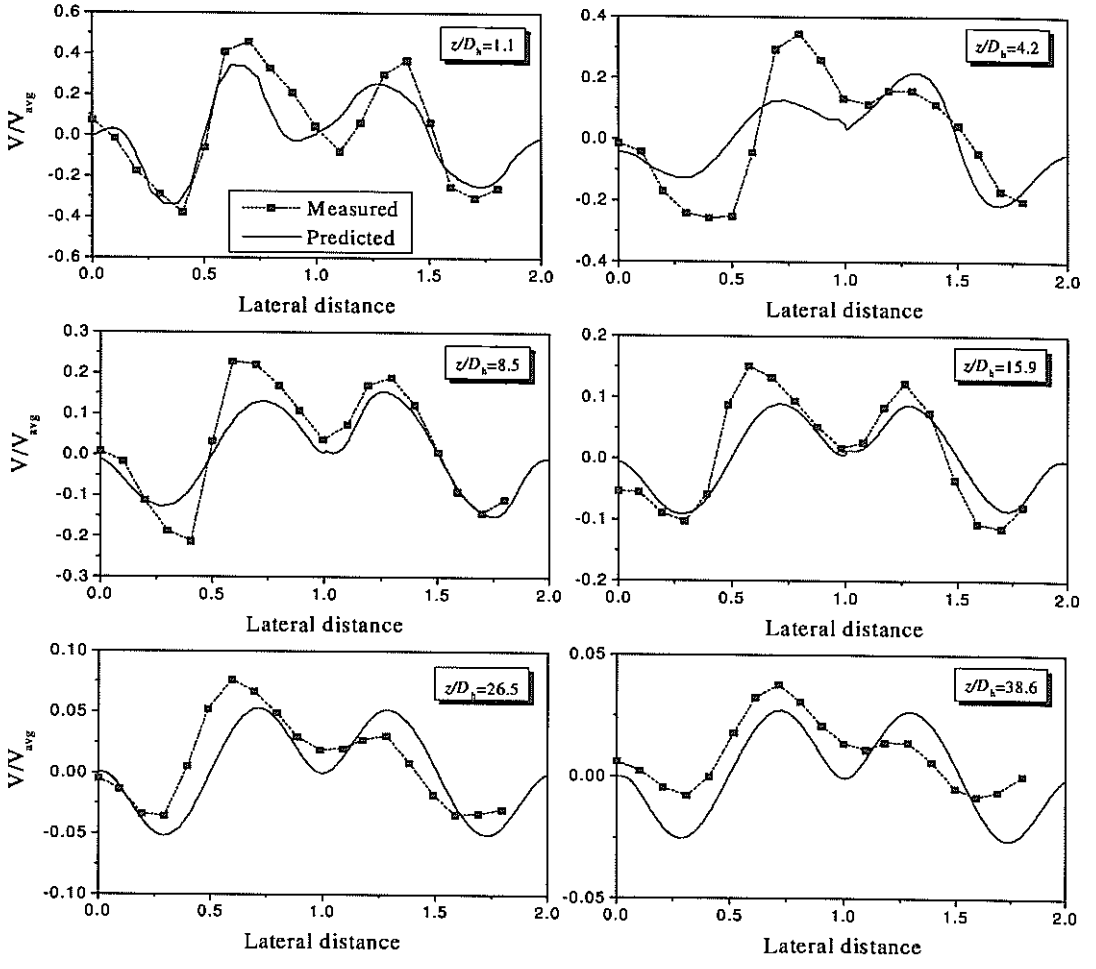

Fig. 5 Lateral velocity along the centerline across two subchannels for split vane

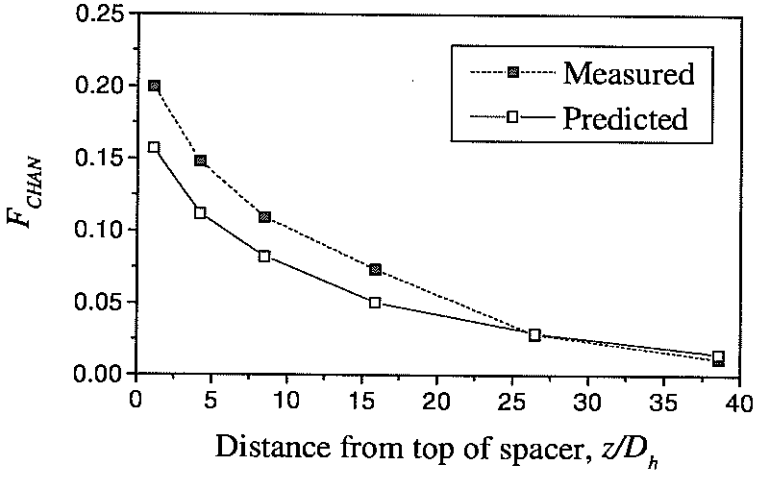

Fig. 6 Swirl ratio in subchannel for split vane

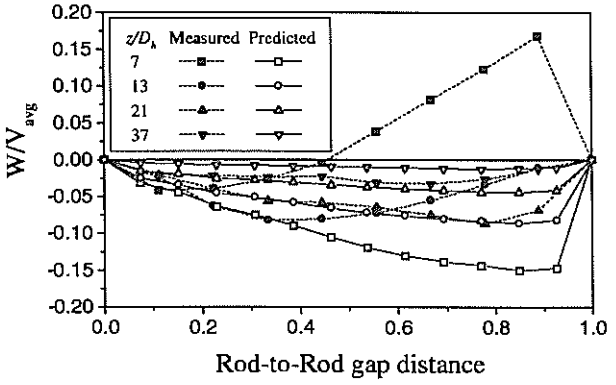

Fig. 7 Transverse velocity distributions on a rod gap region for ripped-open blades

Turbulence Parameters

Figure 8 shows the variation of turbulent kinetic energy at the center of subchannel and the rod gap for the split-vane design. The predicted results are also compared with the experimental results (Yang and Chung, 1996). The CFD predictions indicate a significant increase of the turbulent kinetic energy at the leading edge of the spacer. The turbulent kinetic energy predicted at the center of subchannel increased again due to the acceleration of flow by split vane on top of the spacer. It can be therefore confirmed that the spacer and the mixing blade contribute to promote turbulence in subchannel. The turbulent kinetic energy is somewhat over-predicted at the center of subchannel but under-predicted at the rod gap. This is due to the prediction of smaller crossflow between subchannels as confirmed in Fig. 7. Both the predictions and the measurements showed a rapid decrease slightly downstream of the spacer and stayed at a fully developed level at z/D_h=10.

Figure 9 is a comparison of RMS velocities on a rod gap region of central subchannel for the ripped-open blades. The measured RMS velocity is high and flat near the spacer due to the high mixing and the phenomena of velocity inversion. However, the predicted RMS velocity is low at the middle of rod gap and high near the rod surfaces. This difference is considered as a result of using an inaccurate turbulence model for the high mixing in rod gap region. In the average, the RMS velocity is predicted to be low near the spacer but after 21 D_h, the agreement between the predictions and the measurements is good.

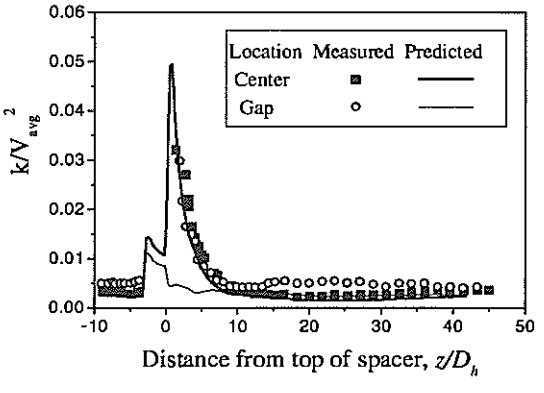

Fig. 8 Axial variation of turbulent kinetic energy for split vane

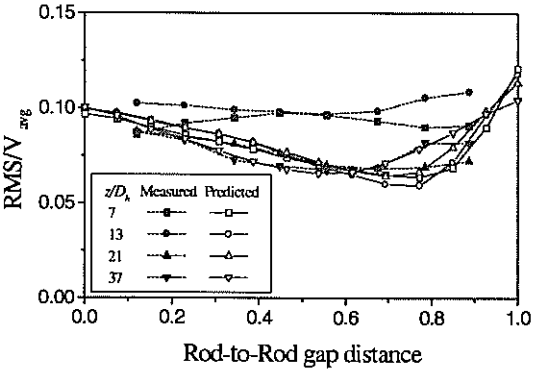

Fig. 9 RMS velocity on a rod gap region for ripped-open blades

CONCLUSIONS

Two experiments with split vane and ripped-open blades were simulated in this CFD study. Both the split vane and ripped-open type mixing promoters have two mixing blades on top of the spacer and bent in opposite directions. The CFD predictions were compared with the measurements to evaluate the CFD application to the nuclear fuel-spacer design. Both the axial and lateral mean velocities predicted by the CFD method showed good agreement with the measurements except for the axial velocity near the spacer with the split vane. The CFD predictions produced the swirling flow pattern in subchannel for the split-vane design and the crossflow mixing between subchannels for the ripped-open blades. The high swirl in subchannel (split vane) and the crossflow mixing (ripped-open blades) occurred close to the spacer but rapidly changed to the axially dominant flow downstream of the spacer. It was also confirmed that the turbulence in subchannel was significantly promoted by the spacer and the mixing devices but rapidly decreased to a fully developed level approximately 10 times of hydraulic diameter downstream of the top of the spacer. The CFD predictions in this study well presented the 3-D turbulent flow characteristics in subchannel of rod bundles with mixing devices. It is therefore expected that the CFD method is quite effective for developing the optimal design of grid spacers with the mixing devices.

ACKNOWLEDEMENT

The authors express their appreciation to the Ministry of Science and Technology (MOST) of Korea for financial support.

REFERENCES

1. Rowe D.S., Johnson B.M. and Knudsen J.G., "Implications Concerning Rod Bundle Crossflow Mixing based on Measurements of Turbulent Flow Structure," *Int. J. Heat Mass Transfer*, Vol. 17, 1974, 407-419.
2. Moller S.V., "On phenomena of turbulent flow through rod bundles," *Exp. Thermal and Fluid Science*, Vol. 4, 1991, 25-35.
3. Rehme K., "The structure of turbulence in rod bundles and the implications on natural mixing between the subchannels," *Int. J. Heat Mass Transfer*, Vol. 35, 1992, 567-581.
4. Shen Y.F., Cao Z.D. and Lu Q.G, "An investigation of crossflow mixing effect caused by grid spacer with mixing blades in a rod bundle," *Nuclear Engineering and Design.*, Vol. 125, 1991, 111-119.
5. Yang S.K. and Chung M.K., "Spacer grid effects on turbulent flow in rod bundles," *J. of the Korean Nuclear Science*, Vol. 28, 1996, 56-71.
6. Imaizumi M., Ichioka T., Hoshi M., Teshima H., Kobayashi H. and Yokoyama T., "Development of CFD Method to evaluate 3-D Flow Characteristics for PWR Fuel Assembly," *Trans. of the 13th Int. Conf. on SMiRT*, Porto Alegre, Brazil, August, 1995.
7. Karoutas Z., Gu C.Y. and Scholin B., "3-D Flow Analyses for Design of Nuclear Fuel Spacer," *Proc. of the 7th Int. Meeting on Nuclear Reactor Thermal-Hydraulics*, Newyork, United Sates, September, 1995.
8. AEA Technology, CFX-4.2 Solver, Harwell Laboratory, Oxfordshire, UK, 1997.
9. Launder B.E. and Spalding D.B., "The numerical computation of turbulent flows," *Computational Methods in Applied Mechanics and Engineering*, Vol. 3, 1974, 269-289.